RESEARCH ARTICLE

Neem-assisted Green Synthesis and Multi-technique Characterization of CuO Nanoparticles for Sustainable Applications

Sanjeev Kumar[1], **Gurjinder Singh**[2,*] **and Jyoti Gaur**[3,*]

[1] Department of Physics, Chandigarh University, Mohali 140413, India
[2] Department of Electrical and Electronics and Communication Engineering, DIT University, Dehradun 248009, India
[3] Research and Incubation Centre, Rayat Bahra University, Punjab 140301, India

Abstract

In the present work, copper oxide (CuO) nanoparticles have been synthesized by a greener and more sustainable approach from neem (Azadirachta indica) leaf extract, which acts as a natural reducing and stabilizing agent. The phase composition, structural, and morphological features of the nanomaterial were thoroughly characterized by XRD, FTIR, UV-Vis spectroscopy, FESEM, TEM, and EDS. X-ray diffraction confirmed the monoclinic formation of CuO with an average crystallite size of 16.68 nm, while FTIR spectra showed Cu-O lattice vibrations and relevant functionalities of phytochemical capping. Optical studies exhibited a unique absorption peak at 350 nm and direct band gap of 2.7 eV that indicate photocatalytic and optoelectronic potentials. The FESEM images revealed nanoflake petal-like morphology with sizes below 100 nm, while EDS mapping showed the elemental purity of the final product. TEM analysis indicated polygonal particles in the range of 60–90 nm with exposed lattice fringes confirming polycrystalline structure composed of smaller crystallites resolved by XRD. The findings indicate that neem-mediated synthesis is an eco-friendly approach to fabricating CuO nanoparticles with biofunctionalized features possessing well-defined crystallinity, morphology, and surface chemistry, which can be applied in catalysis and drug-plant interactions for potential applications in medicine (via biofunctionalized features), photocatalysis, and antimicrobial activities, contributing to sustainable environmental and pharmaceutical technologies.

Keywords: green synthesis, CuO nanoparticles, neem extract, hydrothermal method, phytochemical reduction, photocatalysis, structural and morphological characterization.

1 Introduction

Copper oxide (CuO) nanoparticles are one of the most popular p-type semiconductors studied today,

Submitted: 05 October 2025
Accepted: 24 December 2025
Published: 30 December 2025

Vol. 1, **No.** 2, 2025.
10.62762/TAFMP.2025.440766

***Corresponding authors:**
✉ Gurjinder Singh
gurjinderrsingh@yahoo.com
✉ Jyoti Gaur
gaurj36@gmail.com

Citation
Kumar, S., Singh, G., & Gaur, J. (2025). Neem-assisted Green Synthesis and Multi-technique Characterization of CuO Nanoparticles for Sustainable Applications. *ICCK Transactions on Advanced Functional Materials and Processing*, 1(2), 58–67.

© 2025 by the Authors. Published by Institute of Central Computation and Knowledge. This is an open access article under the CC BY license (https://creativecommons.org/licenses/by/4.0/).

with their narrow band gap (1.2–1.9 eV) and high exciton binding energy (∼17 meV) making them useful in photocatalysis [1] , solar cells, supercapacitors, sensors, and even biomedical platforms [2] . Notably, CuO nanoparticles possess a significantly larger surface area-to-volume ratio, defect density, and surface reactivity compared to bulk CuO, allowing for improved catalytic and antimicrobial properties. For instance, it was determined that CuO nanoparticles had antimicrobial inhibition zones greater than 18–22 mm against *Staphylococcus aureus* at 50 μg/mL [3] , while CuO nanoparticles reached 97% methylene blue photodegradation within 90 minutes via dye degradation processes under visible light irradiation at 100 mW/m^2 [4] . However, conventional nanomaterial synthesis usually employs chemical approaches with toxic reductants (i.e., sodium borohydride, hydrazine hydrate, ethylene glycol) and higher calcination temperatures (>400 °C), thus increasing the final cost of production and energy expenditure as well as creating toxic by-products that reduce practicality across nanotechnology sustainability efforts as well as direct biomedical applications [1, 5].

Therefore, green synthesis approaches have emerged as easily accessible, environmentally friendly, cost-effective, and biocompatible alternatives. Among the many biological templates available (plants, bacteria, fungi, algae), neem (Azadirachta indica) is one of the most common due to its high availability across geographies and phytochemical diversity [6, 7]. Neem leaves contain over 140 biologically active compounds, including azadirachtin ($C_{35}H_{44}O_{16}$), nimbin ($C_{30}H_{36}O_9$), quercetin ($C_{15}H_{10}O_7$), nimbolide ($C_{27}H_{30}O_7$), and numerous terpenoids and flavonoids [6, 8].

For comparison, other green synthesis routes using extracts from plants like aloe vera and Moringa have also been explored. However, these often need larger crystallite sizes or less stable dispersions due to limited functional groups available for metal ion reduction and capping. In contrast, the neem provides a diverse combination of terpenoids, flavonoids, and limonoids that enable stronger chelation and better control of nucleation and growth, resulting in more uniform and crystalline CuO NPs.

These molecules are known for their antioxidant, antibacterial, antiviral, and anticancer properties and act as reducing agents (Cu^{2+} ions reduced to form CuO nuclei) and stabilizing/capping agents (prevent agglomeration/increased colloidal stability) [9, 10]. For example, the flavonoid quercetin has abundant hydroxyl groups (-OH), which act to bind nanoparticles together, while the terpenoid azadirachtin has multiple ester and carbonyl groups, which can chelate and bond to nanoparticle surfaces for moderated nuclear growth [11].

In addition to the chemical rationale, neem's strategic benefits extend to sourcing and global availability. India boasts ∼4.8 million tons of neem leaves produced annually, with neem trees proliferating across regions of Asia, Africa, and even Tropical America, ensuring consistent annual availability. In systems of traditional medicine like Ayurveda, neem derivatives have been used for generations to treat dermal maladies and anti-inflammatory, suggesting innate biocompatibility and therapeutic symbiosis [8]. Relative to other plant templates like Aloe vera or Ocimum sanctum, neem-mediated consistently yield smaller crystallite sizes (typically <30 nm) and improved dispersion relative to other mediating agents, which can be explained by the availability of multifunctional biomolecules within neem extracts [12, 13]. Thus, neem serves as a plentiful and economically feasible green precursor but also a biomedically active contributor that serves to increase the functional value of CuO nanoparticles. Therefore, the neem-assisted green synthesis of CuO nanoparticles manifests multiple advantages through (i) an eco-benign approach eliminating hazardous reagents, excess energy requirements, and complications with downstream environmental impact and (ii) simultaneously biologically-induced arrival of bioactive capping agents for stabilization, biocompatibility, and added biological potential. Such a combination of strategic approaches makes the neem-mediated CuO nanoparticles synthesis process one with high translational potential and significant success due to biosource availability, related performance efficacy, and bridging dissimilar fields of nanomaterials engineering with biomedical or environmental approaches from the onset.

While many plant extracts have been utilized in the green synthesis of CuO nanoparticles thus far, many reported syntheses result in larger crystallite sizes (>40 nm), non-full phase purity findings, or incomplete characterizations [14]. Furthermore, neem (Azadirachta indica) possesses over >140 identifiable bioactive components yet has seldom been systematically explored for its comprehensive reductive and stabilizing capacities of CuO nanoparticles. In addition, much available

work relies on 1 or 2 techniques validated but does not compile structural (XRD), morphological (SEM/TEM), optical (UV–Vis), and chemical (FTIR) into an inclusive series, rendering findings less reproducible and lacking a more thorough understanding of the functional contribution of neem in nanoparticle creation. Although several studies have reported the green synthesis of CuO nanoparticles using various plant extracts, many of them lack complete characterization or yield larger crystallite sizes (> 30 nm) with mixed phases and irregular morphologies. Furthermore, there is a limited quantitative correlation between the phytochemical composition of neem extract and its influence on CuO structure, morphology, and band gap. To address these gaps, the present work focuses on neem-mediated hydrothermal synthesis of CuO NPs with comprehensive multi-technique characterization to establish a clear link between synthesis conditions, structural parameters, and potential functional applications.

The aim of the present work is therefore to synthesize CuO nanoparticles using neem leaf extract as a green route and to comprehensively characterize them using XRD, SEM, TEM, UV–Vis, and FTIR. The study aims to confirm the phase–purity of monoclinic CuO, evaluate the crystallite size and particle morphology, determine the optical band gap shifts, and identify the phytochemical groups responsible for nanoparticle capping. By correlating these results, the work aims to establish neem as a sustainable and biologically active template for the synthesis of CuO nanoparticles. Unlike earlier neem-based CuO syntheses, this work demonstrates improved crystallinity (16.68 nm), controlled nanoflake morphology (60–90 nm), and higher band gap (2.7 eV) through optimized hydrothermal conditions, establishing its distinct novelty.

2 Methodology

2.1 Materials

Copper (II) nitrate trihydrate ($Cu(NO_3)_2{\cdot}3H_2O$) (M.W. = 241.63 g·mol^{-1}, purity 98%, Sigma-Aldrich) was used as the copper precursor. Fresh leaves of Azadirachta indica (neem) were collected locally, washed thoroughly, and shade-dried before extraction. Analytical grade ammonia solution (25%, Merck) was employed to adjust the pH during synthesis. Double-distilled water (DDW) was used throughout the experimental procedures to ensure purity and prevent contamination.

2.2 Method

2.2.1 *Extraction of Neem Leaf Phytochemicals using Soxhlet*

About 20 g of fresh Azadirachta indica (neem) leaves were collected and extensively washed with tap water and subsequently with double-distilled water to remove dirt and other surface impurities. Thereafter, the leaves were shade dried at room temperature (28–30°C) until constant weight was observed. The dried leaves were powdered coarsely using a sterile mechanical grinder.

For extraction, the powdered material was placed in a cellulose thimble which was set in a Soxhlet apparatus. A total of 200 ml of double-distilled water was used as the extraction solvent in the Soxhlet unit maintained at 80°C for 50 minutes to ensure maximum breakdown of cellular compartments and release of soluble phytochemicals into the solvent, as well as exhaustive extraction without thermal degradation of active biomolecules. At the end of the procedure, the extract was decanted, brought to room temperature (25–27 °C), and filtered through Whatman No. 1 filter paper to separate excess plant materials. An approximate volume of 50 mL of clear aqueous extract was obtained, which contained various phytoconstituents, including azadirachtin, nimbin, nimbolide, quercetin, and flavonoids that would act as a reducing and stabilizing agent in the subsequent synthesis of CuO nanoparticles. The extract was kept for further use in amber glass containers at 4 °C.

2.2.2 *Synthesis of CuO Nanoparticles*

Copper oxide nanoparticles were synthesized using aqueous extract of Azadirachta indica leaves as a biogenic reducing and stabilizing agent. For example, 1 g of Copper(II) nitrate trihydrate ($Cu(NO_3)_2{\cdot}3H_2O$) was taken in a vessel and added to 45 mL of double-distilled water. The copper salt was dissolved under magnetic stirring for 15 minutes to obtain a uniform precursor solution. Subsequently, the precursor solution was added dropwise to 40 mL of freshly prepared neem leaf extract under magnetic stirring for 10 minutes. The pH of the freshly prepared neem leaf extract was 5.5, and upon adding copper nitrate solution, it increased to 6.5. To increase the nucleation of CuO nanoparticles, the pH of the reaction mixture was adjusted to 9.5 by adding ammonia solution (25%) dropwise. The resultant well-mixed solution was transferred to a Teflon-lined stainless-steel autoclave, closed tightly, and subjected

to hydrothermal treatment at 160 °C for 20 hours in a laboratory oven. After completion, the autoclave was cooled naturally to room temperature (25–27 °C), and a dark-colored suspension was formed. These hydrothermal parameters (160 °C for 20 h) were selected after preliminary trials in the 120-160 °C for 20 h, produced the most uniform nanoflake morphology with phase-pure monoclinic CuO and minimal agglomeration. Lower temperatures or shorter durations resulted in incomplete conversion, while higher values led to irregular grain growth and particle fusion.

In order to precipitate out the obtained nanoparticles, the suspension was subjected to centrifugation at 10,000 rpm for 12 minutes, followed by a second centrifugation of 10 minutes. The resultant solid product was washed with double-distilled water and ethanol to remove excess phytochemicals or remaining ions in the mixture and then filtered through Whatman No.1 filter paper. The obtained materials were dried at 80 °C for 6 h and finally ground using an agate mortar and pestle to obtain a fine black powder of neem-mediated CuO NPs. The dried powder was subjected to calcination in a muffle furnace at 400 degrees Celsius for 1.5 h under air conditions. Thus, after calcination, a fine black powder of copper oxide nanoparticles was obtained and stored in a desiccator until characterization and further use. Therefore, this simple and reproducible route produced phase-pure CuO nanoparticles where the neem phytochemicals acted as simultaneous reducing agents (reducing Cu^{2+} into CuO nuclei) and capping agents (preventing agglomeration) to provide high stability and homogeneity of the final product.

As shown in Figure 1, the mechanism of phytochemical-assisted reduction and formation of CuO NPs can be represented as follows:

$$Cu(NO_3)_2 3H_2O \rightarrow Cu^{2+} + 2NO_3^- + 3H_2O \quad (1)$$

$$Cu^{2+} + \text{Phytochemicals (flavonoids, terpenoids, polyphenols)} \rightarrow Cu(OH)_2 \rightarrow CuO + H_2O \quad (2)$$

Here, the hydroxyl and carbonyl groups of neem-mediated biomolecules donate electrons to reduce Cu^{2+} ions, while carbonyl and ester moieties form complexes that stabilize the nucleated CuO NPs.

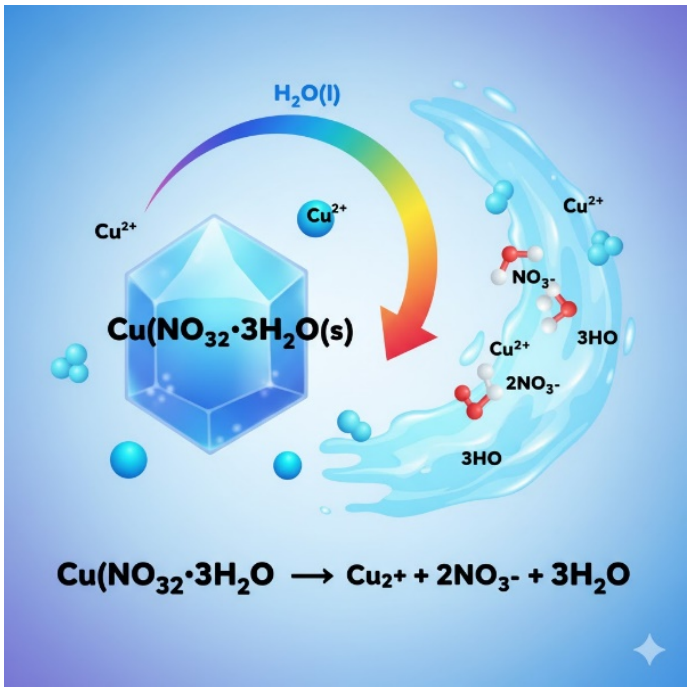

Figure 1. Dissociation of $Cu(NO_3)_2{\cdot}3H_2O$ and formation of Cu^{2+} ions.

2.2.3 *Characterization Methods*

The structure of the synthesized CuO NPs was determined by X-ray diffraction (XRD) using Bruker D8 Advance diffractometer (Cu Kα radiation, λ = 1.5406 Å, 40 kV, 30 mA). The instrument was calibrated using a standard silicon sample before measurements to ensure accuracy. UV-Vis absorption spectra were recorded with JASCO-715 spectrophotometer (wavelength range 200-800 nm) using a baseline correction with pure solvent reference. FTIR spectra were collected with a Bruker Alpha II FTIR spectrometer using KBr Pellets. Field emission scanning electron microscopy (FESEM) images were obtained using JEOL JSM-7610F Plus microscope operated at 5 kV. Transmission electron microscopy (TEM) was performed using a FEI Tecnai G2 F20 instrument at 200 kV, with lattice spacing validated against standard CuO JCPDS data for calibration.

3 Results and Discussion

3.1 X-ray Diffraction (XRD) Analysis of CuO Nanoparticles

To explore the structural properties of CuO nanoparticles prepared from neem extract, X-ray diffraction (XRD) studies were conducted. The XRD pattern was obtained over the 2θ range of 20°–80° (Figure 2), where all peaks were in accordance with monoclinic CuO from the data bank JCPDS (Card No. 00-089-2531), verifying the formation of tenorite

with no other impurity reflections of Cu_2O or metallic copper being evident, in accordance with high-phase purity performance under phytochemical-mediated reduction and capping. The strongest Bragg reflections registered at $2\theta \approx 32.50°$, 35.60°, and 38.68° corresponding to the (110), (002), and (111) planes, respectively. Higher angle reflections were attributed to (−112), (−202), (020), (202), (−113), (022), (220), (−312) and (−222). Peaks are characterized by their sharpness and symmetry, suggesting crystallization, while the relative intensities of the peaks confirm that (110), (002), and (111) planes are more oriented than others in the crystalline phase. The size of crystallites was determined from the Debye–Scherrer equation:

$$D = \frac{K\lambda}{\beta \cos\theta} \tag{3}$$

where K = 0.9; λ = 1.5406 Å; β = full width at half maximum in radians. The sizes ranged from 3.57 nm (−222) to 37.24 nm (−112) with an average crystallite size of ∼16.68 nm. Notably, the most intense reflections ((002) and (111)) exhibited relatively narrower peaks, corresponding to larger crystallite sizes (∼10-11 nm) within the sample, while broader peaks at higher angles (e.g., (-222)) indicated smaller coherent domains (∼3-6 nm). This variation suggests the presence of size anisotropy or microstrain within the polycrystalline nanoparticles. On the other hand, reflections corresponding to higher angles showed large widths, indicating a higher level of strain formation and thus lower coherency lengths in these directions.

Table 1. XRD data of CuO nanoparticles synthesized using neem extract.

2θ (degree)	FWHM B (DEGREE)	d-spacing	Crystallite Size (D) (nm)
32.5	0.65821	2.75275	13.13
35.6	0.80087	2.51983	10.88
38.68	0.86634	2.32597	10.15
46.04	0.24207	1.96981	37.24
49.02	0.96593	1.85681	9.44
51.6	0.28448	1.76986	32.40
53.06	0.85508	1.72455	10.85
58.26	0.60755	1.58240	15.63
61.46	0.92114	1.50746	10.48
65.9	1.0137	1.41623	9.75
67.94	0.92959	1.37859	10.76
72.12	1.92959	1.30863	5.32
74.98	2.92959	1.26564	3.57
		Average Size = 16.68 nm	

Interplanar spacings (d) were concurrently calculated via Bragg's equation:

$$n\lambda = 2d \sin\theta \tag{4}$$

The calculated d-spacings (Table 1) ranged between 2.7528 Å and 1.2656 Å, which were highly comparable to values found in CuO standards as well. Deviations from peak width and position are attributed to phytochemical surface passivation as well as lattice microstrain induced during the green synthesis of CuO nanoparticles. These results confirm that the neem-mediated hydrothermal route not only preserves structural integrity but also promotes the formation of phase-pure, highly crystalline CuO nanoparticles with average domain sizes around 16.68 nm, which are suitable for nanoscale functional applications. The obtained average crystallite size (∼ 16.68 nm) is significantly smaller than values reported for CuO synthesized using Aloe Vera (∼ 25 nm) and Moringa oleifera (∼ 28 nm) extracts [12, 14], highlighting the superior size control and crystallinity achieved via neem-mediated hydrothermal synthesis.

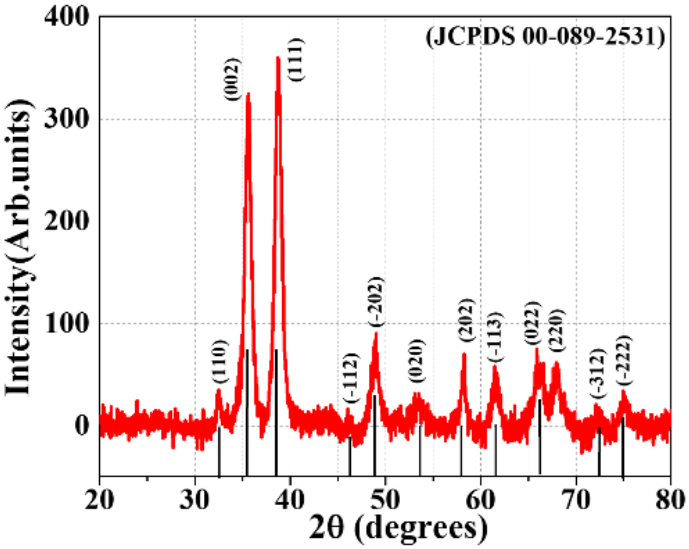

Figure 2. XRD pattern of neem-mediated CuO nanoparticles compared with the standard JCPDS card (No. 89-2531), confirming monoclinic CuO phase.

3.2 UV–Visible Spectroscopy Analysis

UV–Visible spectroscopy was utilized to probe the optical properties and band-gap response of neem-mediated CuO nanoparticles. As shown in Figure 3, the UV–visible absorption spectrum recorded in the 200–800 nm range presents a well-defined, sharp absorption peak located at 350 nm for CuO, corresponding to ligand-to-metal charge transfer (O^{2-}

$\rightarrow Cu^{2+}$) during electronic transitions within the CuO lattice and influenced by phytochemical capping material from the neem extract. Such transitions are typical of nanocrystalline CuO and represent strong electron coupling within the metal oxide and with biologically active compounds.

The spectrum also demonstrates a continuous absorption tail toward the visible region typical of semiconductors. The optical band gap (E_g) was calculated according to Tauc's relation:

$$(\alpha h\nu)^y = A(h\nu - E_g) \quad (5)$$

in which α represents the absorption coefficient, $h\nu$ the photon energy, A the proportionality constant, and y is specific to the type of electronic transition. Here, $y = 2$ was used because it corresponds to a direct allowed transition. Therefore, the Tauc plot of $(\alpha h\nu)^2$ versus $h\nu$ was constructed, and extrapolation of the linear region to $(\alpha h\nu)^2 = 0$ yielded an optical band gap (E_g) of 2.7 eV.

This value is significantly greater than the E_g of bulk CuO (~1.7 eV) which corresponds to a blue shift of nearly 1.0 eV, which is representative of quantum confinement effects when particle size equals dimensions on the exciton Bohr radius. This finding supports the crystalline domain sizes determined by XRD (~16 nm), confirming that as synthesized are indeed particles in the nanometer size range. Furthermore, the lack of secondary peaks ascribed to other copper oxides confirms that no Cu_2O or metallic copper contributes to the crystallization.

Overall, UV–Vis confirms that these particles are quantum confined CuO nanoparticles with greater band-gap energy as produced through this neem-assisted hydrothermal approach. Such properties are favorable for photocatalysis and optoelectronic applications. The obtained band gap of 2.7 eV is slightly higher than that reported for chemically synthesized CuO [1, 13] and marginally above values from green routes such as Aerva javanica [5] and Tribulus terrestris [2]. This blue shift confirms the role of neem phytochemicals in restricting grain growth and enhancing surface energy during nucleation, leading to smaller crystallites and stronger quantum-confinement effects.

3.3 Fourier Transform Infrared (FTIR) Spectroscopic Characterization of Neem-Mediated CuO Nanoparticles

Fourier-transform infrared spectroscopy (FTIR) analysis was performed to investigate surface chemistry and confirm the contributions of phytochemical functionalities from neem extract in the reduction and stabilization of CuO nanoparticles (Figure 4). The FTIR spectrum shows a broad absorption range of 3746 to 2650 cm^{-1}. The inset of the spectrum shows broader and sharper peaks located at 3746, 3780, 3025, 2980, 2886, and 2650 cm^{-1}, which are reported for O-H and C-H stretching modes. The sharper bands around 3746 and 3780 cm^{-1} correspond to symmetric and asymmetric stretching of hydroxyl (-OH) groups, suggesting the adsorption of phenolic or flavonoid or alcohol compounds from neem extract. The overlapping peaks found at 2886–2980 cm^{-1} are from aliphatic C–H stretching modes that occur from methyl ($-CH_3$) and methylene ($-CH_2$) groups from terpenoid structures or fatty acid residues comprising the capping medium. The peak detected at 2650 cm^{-1} is a less intense region of stretching that corresponds to stretching vibrations of aldehyde (-CHO) groups, indicating the presence of reducing sugars or another active aldehyde phytoconstituents. In the midregion from 2000–400 cm^{-1}, peaks are attributed to weak overtones or combination modes that occur at 2153, 2116, 2032, and 1917 cm^{-1}; or C≡C or C≡N stretching from trace nitriles or alkynes with little potential for resonance, suggesting partial coverage by plant-derived segments. In the region of fingerprinted detection, the most intense peaks appear at 1492 cm^{-1} and 1367 cm^{-1} due to symmetric and asymmetric stretching of carboxylate ($-COO^-$) groups and possible bending vibrations of $–CH_3$ groups. Strong evidence supports the presence of carboxylic acids or esters that likely contributed significantly to metal ion complexation and reduction during formation. The peak located at a range of 813 cm^{-1} is attributed to Cu–O lattice vibrations and confirms the formation of crystalline CuO nanoparticles. This peak arises from metal–oxygen stretching in the monoclinic crystalline form of CuO consistent with previous reports. The presence of organic functional groups from neem extract throughout the FTIR spectrum confirms the successful bio-functionalization and capping of CuO nanoparticles by plant phytochemicals, which not only facilitated the green synthesis but may also enhance colloidal stability and biological activity of the nanoparticles. The functional groups observed can be directly linked to major phytochemicals present

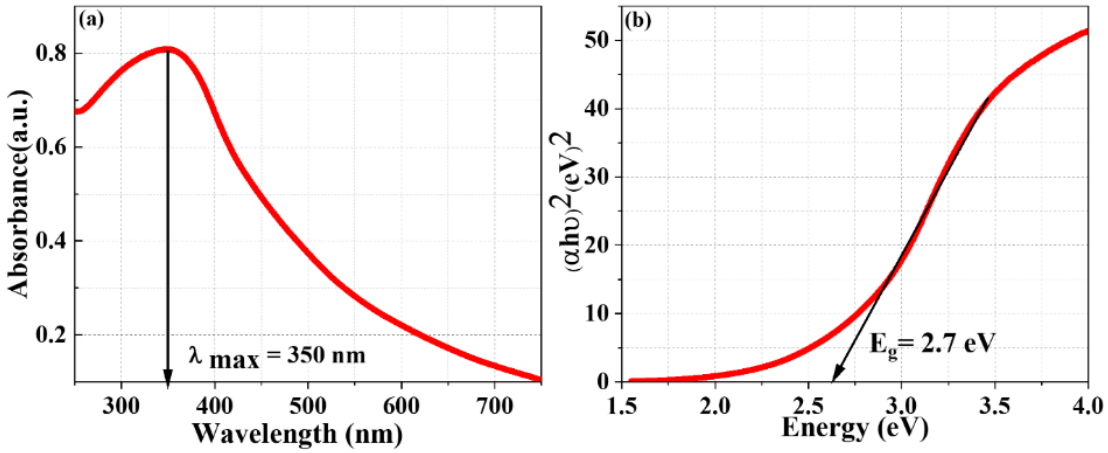

Figure 3. (a) UV–Vis absorption spectrum of neem-mediated CuO nanoparticles showing a strong absorption peak at $\lambda_{max} = 350$ nm. (b) Tauc's plot for direct allowed transition $(\alpha h\nu)^2$ vs $h\nu$ indicates an optical band gap ($E_g = 2.7$ eV).

in neem extract. The O-H and C=O stretching bands correspond to hydroxyl and carbonyl groups in quercetin and nimbolide molecules, while the C-O-C stretching around 1020-1100 cm^{-1} is attributed to azadirachitin and other terpenoids. Similarly, the C-H stretching near 2900 cm^{-1} originates from aliphatic groups of nimbin and fatty acid derivatives. These association indicate that neem phytoconstituents act as both reducing and stabilizing agents during nanoparticle formation.

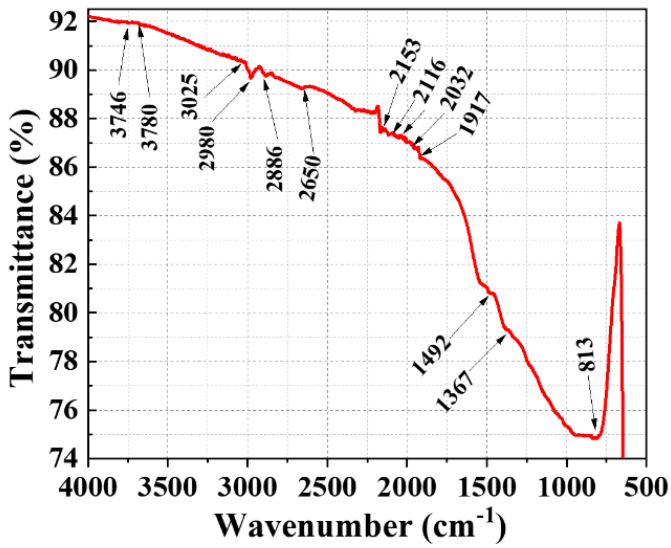

Figure 4. FTIR spectrum of CuO nanoparticles synthesized using neem extract, confirming phytochemical capping and Cu–O bond formation.

3.4 FESEM and EDS Analysis of Neem-Synthesized CuO Nanoparticles

Field emission scanning electron microscopy equipped with energy dispersive x-ray spectroscopy (EDS) analysis for surface morphology and elemental composition was conducted and is shown in Figure 5. SEM micrographs provide high-resolution topographical information about the particles and their size and distribution at varying field sizes. For example, in Figure 5(a), assessed at 50,000× magnification, CuO nanoparticles appear to be agglomerated with densely packed sheet-like but thin platelets with a flower-like morphology. Such sheet-stacked appearances are common in bio-synthesized oxides, and since these particles are not entirely fused, the capping mechanism occurs via biomolecules in the neem extract solution. This is likely due to polyphenolic or flavonoid-like contributions that stabilize the particles post-nucleation. The jagged edges and less-fused connectivity may also produce facet-selective growth. The aggregates appear irregularly shaped but consistently layered, suggesting that these are exposed to each other via lattice expansion to yield a high surface area material with enhanced catalyst or antimicrobial properties—ideal for medical device applications. Particles do not appear fused either, indicating that they are stabilized with capping during synthesis to ensure discrete, independent particles.

A closer magnification view in Figure 5(b) (100,000×) allows the observation of platelets as single entities on their surfaces. A rough surface with edges defines each nanoplate, indicating some level of surface functionalization from the organic moieties supplied by the neem extract. This somewhat rough surface can enhance surface reactivity. No edges appear completely smooth, which could create a mechanically induced edge instead of nanoplate formation through a top-down approach. Thickness measurements yield an average of 20–40 nm for each nanoplatelet, while lateral

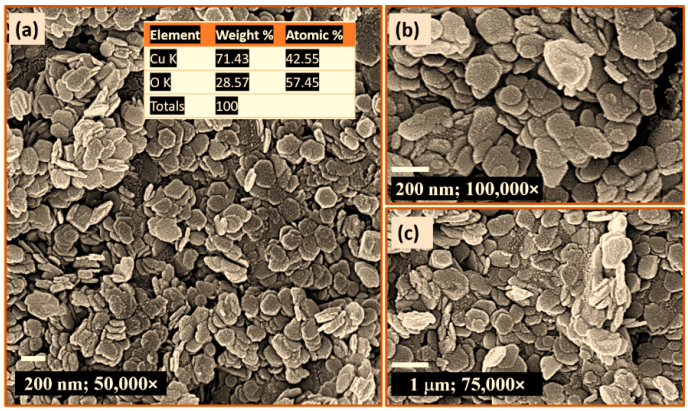

Figure 5. FESEM images of neem-derived CuO nanoparticles at (a) 50,000×, (b) 100,000×, and (c) 75,000× magnifications showing stacked nanoflake morphology; the inset shows EDS confirming Cu and O as the only elements present.

observations range from 50–100 nm, consistent with crystallite size from XRD. The high-resolution image details confirm the nanoscale regime and a relatively consistent morphology within the parameters viewed.

As we shift focus to Figure 5(c) obtained at 75,000× magnification, a wider distribution of CuO nanoflakes is noted. Secondary agglomerates of a larger size can be observed, which can be attributed to weak interparticle interactions exerted during the drying process. However, despite some agglomeration, edges remain distinguishable from one another, indicating that the nanoparticles were not sintered. The combination of an assortment of small flakes and hierarchical stacking into larger conglomerates also indicates that growth occurred heterogeneously in two different fashions, supported by secondary nucleation-coalescence during regulated temperature conditions with reactions stabilized by phytochemicals present in the neem extract.

Finally, the inset of Figure 5(a) shows the EDS elemental analysis attributed to the CuO sample. The measured elemental percentages reveal Cu (71.43 wt%; 42.55 at%) and O (28.57 wt%; 57.45 at%) with no other peaks for foreign elements, supporting the phase purity of the synthesized product. The Cu:O atomic ratio approaches 1:1, which supports the logical formation of CuO as determined by the crystalline structure exhibited via XRD. Other foreign elements were not detected, signifying that the green synthesis process is eco-friendly without any contaminant involvement.

The experimentally obtained Cu: O atomic ratio aligns closely with the theoretical stoichiometric value of 1: 1 for CuO, confirming the composition's accuracy within acceptable instrumental limits. No other elements were detected, reaffirming high purity. Although XPS analysis was not performed in the present study. Future work will include oxidation state verification to further validate the Cu^{2+} state and surface chemical environment.

Thus, FESEM images reveal that neem-induced synthesis drives crystalline formation of CuO nanoparticles with isolated flake morphology, nanoscale growth, and effective dispersion stability. The fact that they truly form in such a way is due to the phytochemicals present, which stabilize not only during subsequent differentiation but also post-synthesis for structural integrity. Coupled with EDS findings for elemental purity, this approach for synthesis renders CuO NPs attractive for catalytic, sensing, and biomedical applications, as subsequent studies show. The observed morphology and particle dimensions (60–90 nm) are consistent with green CuO prepared using *Aerva javanica* ($\sim$ 80 -120 nm) [5] and smaller than those obtained by conventional chemicals routes ($>$ 150 nm) [6, 9], confirming the efficiency of the neem-assisted route in producing finer, well dispersed nanostructures.

3.5 Transmission Electron Microscopy (TEM) Analysis of Neem-Synthesized CuO Nanoparticles

To complement the external morphology, the internal structure and nanostructure of the synthesized CuO NPs were studied via Transmission Electron Microscopy (TEM) depicted in Figure 6. TEM micrographs at low and high magnification provide pertinent information regarding particle shape, dispersion, and crystallinity that validate observations from earlier characterization techniques. For example, CuO NPs shown in Figure 6(a) manifest a predominantly polygonal and quasi-hexagonal morphology with clear angular edges and smooth periphery. They are well dispersed with minimal agglomeration, and average particle sizes suggest the presence of about 60–90 nm sized particles. This non-uniformity is still relatively narrow and indicates significant shape-control since neem phytochemicals added during nucleation are expected to modulate facet-selective growth, both during nucleation and thermal treatment. The polycrystalline nature also suggests minimal impact on subsequent pre-treatments.

A higher magnification image (Figure 6(b)) shows

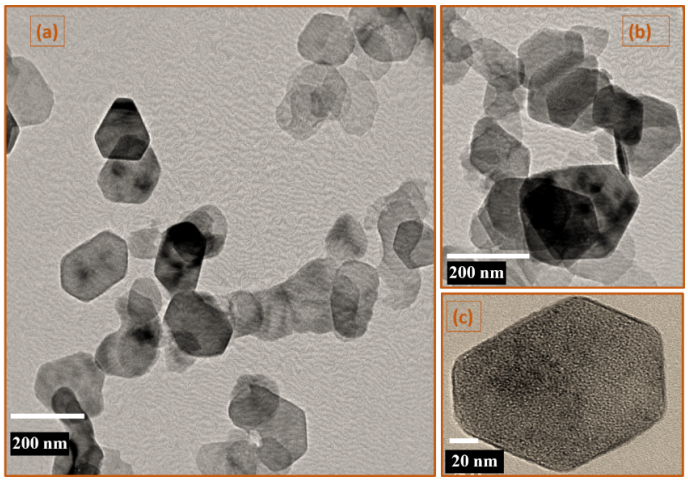

Figure 6. TEM images of CuO nanoparticles showing polygonal morphology and well-defined crystalline structure.

that the angular morphology is retained and the particles appear similarly fused with overlapping edges in certain areas, suggesting that a few crystalline domains coalesced to incorporate into larger uniform scaffolds. This is also observed in Figure 6(c), the high-resolution image—which shows high lattice fringes within a singular particle, suggesting high domain characteristics. The other contrasts are attributed to clearly defined atomic planes that become juxtaposed to macroscopic levels, making it easier to generate average lattice spacing across NPs, leading to the conclusion that they are comprised of crystalline cores consistent with d-spacings associated with monoclinic CuO phases. Interestingly, average particle size based on TEM assessment (60–90 nm) is significantly higher than the crystallite size (∼10–15 nm) based on Debye–Scherrer estimations derived from XRD data, this is somewhat common with nanomaterials and attributed to polycrystalline domains which suggest that the particles seen in TEM are conglomerations of smaller crystallites which have either fused together via the later stages of growth or drying into one single particle which contains several coherent, but individually diffracting, domains. These domains will show up in the width of the peak in XRD, while TEM picks up on the envelope of the particle itself. Thus, both assessments support a core-shell-type polycrystalline structure housing individual crystalline regions or sub-domains stabilized in larger nanostructured bodies by phytochemical capping layers. The TEM results, when correlated with FESEM, XRD, and FTIR findings, confirm the successful green synthesis of high-purity CuO nanoparticles with crystalline internal domains, shape anisotropy, and controlled aggregation behavior, attributes crucial for enhanced surface activity in catalysis and bioapplications. The particle size observed from TEM (60-90 nm) shows good agreement with XRD-derived crystallite dimensions, confirming polycrystalline assembly. The distinctive polygonal morphologies are attributed to the controlled synthesis parameters, especially the pH (9.5) and hydrothermal temperature which prompted uniform nucleation and prevented excessive agglomeration. Such morphologies provide a higher surface-to-volume ratio and active edges sites, enhancing photocatalytic and antibacterial activity of CuO NPs.

4 Conclusion

Thus, this work reports effective, green, plant-mediated synthesis of CuO nanoparticles, with characterizations suggesting neem (Azadirachta indica) extract has acted as a reducing and stabilizing agent. The synthesized CuO NPs exhibited monoclinic crystalline structure, high purity, and uniform morphology, validating the efficiency of the neem-assisted hydrothermal process. Overall, this neem-assisted hydrothermal route provides a cost-effective, reproducible, and environmentally benign approach for synthesizing CuO NPs with controlled size and shape. The process is easily scalable for large-scale production without the use of hazardous reagents or complex instrumentation. Owing to their stable structure, high surface activity, and narrow band gap, the obtained CuO nanoparticles are promising for photocatalytic, antibacterial, and environmental remediation applications.

Data Availability Statement

Data will be made available on request.

Funding

This work was supported without any funding.

Conflicts of Interest

The authors declare no conflicts of interest.

Ethical Approval and Consent to Participate

Not applicable.

References

[1] Keabadile, O. P., Aremu, A. O., Elugoke, S. E., & Fayemi, O. E. (2020). Green and traditional synthesis

of copper oxide nanoparticles—comparative study. *Nanomaterials, 10*(12), 2502. [Crossref]

[2] Meena, J., Kumaraguru, N., Sami Veerappa, N., Shin, P. K., Tatsugi, J., Kumar, A. S., & Santhakumar, K. (2023). Copper oxide nanoparticles fabricated by green chemistry using Tribulus terrestris seed natural extract-photocatalyst and green electrodes for energy storage device. *Scientific reports, 13*(1), 22499. [Crossref]

[3] El-Sherbiny, G. M., Shehata, M. E., & Kalaba, M. H. (2025). Biogenic copper and copper oxide nanoparticles to combat multidrug-resistant Staphylococcus aureus: Green synthesis, mechanisms, resistance, and future perspectives. *Biotechnology Reports*, e00896. [Crossref]

[4] Prakruthi, R., & Deepakumari, H. N. (2024). CuO nanoparticles: green combustion synthesis, applications to antioxidant, photocatalytic and sensor studies. *RSC advances, 14*(39), 28703-28715. [Crossref]

[5] Amin, F., Fozia, Khattak, B., Alotaibi, A., Qasim, M., Ahmad, I., ... & Ahmad, R. (2021). Green synthesis of copper oxide nanoparticles using Aerva javanica leaf extract and their characterization and investigation of in vitro antimicrobial potential and cytotoxic activities. *Evidence-Based Complementary and Alternative Medicine, 2021*(1), 5589703. [Crossref]

[6] Dhakad, A. K., Kumar, R., Choudhary, R., Singh, S., Khan, S., & Poonia, P. K. (2025). Traditional to modern perspectives on Neem (Azadirachta indica): A gateway to bioactive compounds, sustainable agrochemicals and industrial applications. *Industrial Crops and Products, 231*, 121155. [Crossref]

[7] Sarkar, S., Singh, R. P., & Bhattacharya, G. (2021). Exploring the role of Azadirachta indica (neem) and its active compounds in the regulation of biological pathways: an update on molecular approach. *3 Biotech, 11*(4), 178. [Crossref]

[8] Alzohairy, M. A. (2016). Therapeutics role of Azadirachta indica (Neem) and their active constituents in diseases prevention and treatment. *Evidence-Based Complementary and Alternative Medicine, 2016*(1), 7382506. [Crossref]

[9] Mobarak, M. B., Sikder, M. F., Muntaha, K. S., Islam, S., Rabbi, S. F., & Chowdhury, F. (2025). Plant extract-mediated green-synthesized CuO nanoparticles for environmental and microbial remediation: a review covering basic understandings to mechanistic study. *Nanoscale Advances, 7*(9), 2418-2445. [Crossref]

[10] Wylie, M. R., & Merrell, D. S. (2022). The antimicrobial potential of the neem tree Azadirachta indica. *Frontiers in pharmacology, 13*, 891535. [Crossref]

[11] Pasieczna-Patkowska, S., Cichy, M., & Flieger, J. (2025). Application of Fourier transform infrared (FTIR) spectroscopy in characterization of green synthesized nanoparticles. *Molecules, 30*(3), 684. [Crossref]

[12] Yadeta Gemachu, L., & Lealem Birhanu, A. (2024). Green synthesis of ZnO, CuO and NiO nanoparticles using Neem leaf extract and comparing their photocatalytic activity under solar irradiation. *Green Chemistry Letters and Reviews, 17*(1), 2293841. [Crossref]

[13] Khairy, T., Amin, D. H., Salama, H. M., Elkholy, I. M. A., Elnakib, M., Gebreel, H. M., & Sayed, H. A. E. (2024). Antibacterial activity of green synthesized copper oxide nanoparticles against multidrug-resistant bacteria. *Scientific Reports, 14*(1), 25020. [Crossref]

[14] Khalifa, M. J. (2025). Green Synthesis of Copper Oxide Nanoparticles Using Urtica Dioica Leaf Extract. *Journal of Multidisciplinary, 5*(01), 1-4. [Crossref]

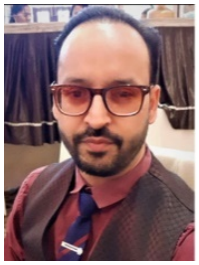

Dr. Sanjeev Kumar is Associate Professor of Physics at Chandigarh University, Mohali, where his research focuses on experimental condensed matter physics, especially superconductivity and magnetism in bulk and low-dimensional materials. He earned his M.Sc. in Electronics (as a gold medalist) and Ph.D. in Materials Science. Over his career, he has published more than 100 research papers, 4 patents and works on novel materials and electronic phenomena at low temperatures. He collaborates broadly and has developed synthesis protocols for diverse nanostructures applied to fields like gas sensing, catalysis and electronics. (Email: Kumarpanju25@gmail.com)

Dr. Gurjinder Singh is an Associate Professor in the Department of Electrical & Electronics & Communication Engineering at DIT University, Dehradun, having joined in July 2023. He holds a Ph.D. in ECE from Desh Bhagat University and an M.Tech from Panjab University. With nearly two decades of experience in teaching, research, and industry, his specialization lies in nanoelectronics and the optical and electronic properties of metal-oxide semiconductor nanomaterials. His research spans chemical and green synthesis methods, photoluminescence, photocatalysis, and device applications. He teaches courses such as Analog Integrated Circuits, Nanoelectronics, and Optical Fiber Communication. (Email: gurjinderrsingh@yahoo.com)

Dr. Jyoti Gaur is Research Assistant Professor at Rayat-Bahra University, where she works in the Research & Innovation Cell. She holds a Ph.D. in Materials Science and focuses on green synthesis of metal-oxide nanomaterials and their environmental/photocatalytic applications. She has published over 30 research papers in her field. Her work seeks to bridge fundamental materials science with real-world environmental solutions. (Email: gaurj36@gmail.com)